# *MPC based path tracking control for autonomous vehicle with multi-constraints*

Mengyuan Chen
College of Information Engineering
Chongqing Vocational Institute of Engineering
Chongqing, China
cmy0904@live.cn

Yue Ren
A) State key laboratory of mechanical transmission
Chongqing University
Chongqing, China
B) Department of mechanical and mechatronics engineering
University of Waterloo
ON, Canada
renyueok@hotmail.com

***Abstract*—In this paper, a nonlinear model predicted control algorithm is proposed for an autonomous vehicle with the known road information which is described by road curvature. The single track vehicle dynamic model is established and vehicle future state is predicted during the predict horizon. To minimize the tracking error, the standard quadratic cost function is proposed to calculate the optimal steering wheel and longitudinal force. Meanwhile, the anti-side slide and anti-rollover speed limit are considered into the constraint of the optimization. The simulation result illustrates that the proposed model predicted control has satisfactory path tracking performance and prevents the vehicle from unstable under different road conditions.**

***Keywords—autonomous vehicle; path tracking; model predictive control***

## I. INTRODUCTION

In past decade, due to the rapid development of control theory and computer science, a plenty of advanced driver assistant systems(ADAS), such as adaptive cruise control(ACC), lane keeping assistance(LKA), and automatic parking assistance(APA), have been carried out to improve the vehicle safety, comfort and aid the drivers in difficult and tedious tasks. However, these systems can be only called 'partial autonomy'[1],[2]. The eventual development of ADAS is the fully automatic vehicle that could totally replace drivers' operation. As the fundamental function of the autonomous vehicle, path tracking control has become the hot research spot around the world these years.

The path tracking problem has been widely researched in robotics and autonomous vehicle [3]. Several control algorithm such as PID control, LQR control and sliding control have been adopted into the path tracking problem[4],[5]. Compared with these control algorithms, model predictive control(MPC) can be used in different levels of the process control structure and is also able to handle a wide variety of process control constraints systematically[6],[7],[8].

This paper proposed the path tracking control framework for the autonomous vehicle based on model predictive control. First, the vehicle nonlinear dynamic model is established and it is linearized by the first order Euler method. The steering wheel angle and longitudinal force are considered as the decision variables to establish the optimization problem to minimize the tracking error. With the known reference trajectory, the convex cost function is formulated which could be transferred into QP problem to obtain the global optimal solutions. Considering the vehicle lateral stability, the anti-sideslip and anti-rollover constrains are also added into the optimization to ensure the vehicle don't lose control under different conditions.

This paper is organized as follows. Section II introduces the description of the reference trajectory. In section III the vehicle model and the control framework of MPC is designed. The simulation results are analyzed in section IV and the conclusion is summarized in section V.

## II. REFERENCE TRAJECTORY

The reference trajectory is the prerequisite for the path tracking problem which leads the autonomous vehicle to its destination. The path planning problem includes global path planning and local path planning. The global path planning generates the road map according to the road shape detected by HD map, which calculates the optimal path to the destination. And the local path planning is to establish the local collision avoidance trajectory based on the vehicle sensors such as radar and camera. Due to the rapid change of the environment, the local path planning requires high computing speed. In this paper, it is assumed that the reference trajectory has been planning already, which could be expressed as:

$$\psi(s) = \int_0^s K(s)ds + \psi_0 \quad (1)$$

$$X(s) = \int_0^s \cos\psi(s)ds + X_0 \quad (2)$$

$$Y(s) = \int_0^s \sin\psi(s)ds + Y_0 \quad (3)$$

where the initial longitudinal position, lateral position and heading angle of the vehicle are $X_0, Y_0, \psi_0$, respectively. $K(s)$ represents the road curvature, which is expressed as the function of distance $s$ [9]. When $K(s)=0$ the road is totally straight and if the road is curved, the $K(s)=1/R$,

978-1-5386-2602-3/17/$31.00/ ©2017 IEEE

where $R$ is the radius of the curved road. It can be seen from equation (1)-(3) that the reference trajectory provides the vehicle position information – including longitudinal position, lateral position, road curvature and heading angle.

## III. PATH TRACKING CONTROLLER

The overall control architecture is shown in Fig.2. With the current vehicle state, the NMPC predicts the future state during the predict horizon. And the optimizer calculates the optimal control input with constraints which gives the minimum value of the cost function. At last, the control distribution block calculates the real control input of each actuator of the vehicle such as steering wheel angle and driven/brake torque of each wheel motor.

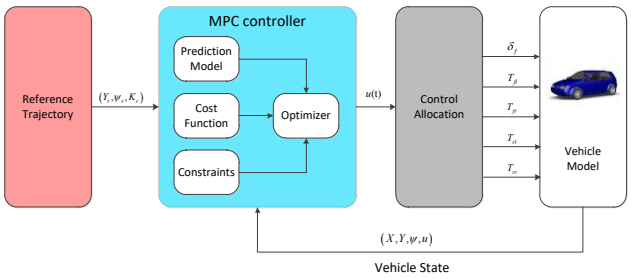


Fig. 1. The overall control architecture

### A. Vehicle Model

In this section, the vehicle model used for path tracking controller is described. For MPC controller, a 3-DOF nonlinear extended bicycle model is adopted here, which is shown in Fig.2.

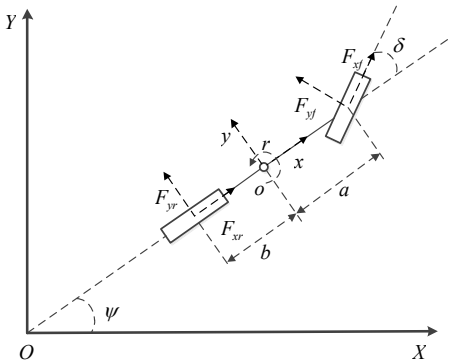


Fig. 2. The vehicle dynamic model

By using Newton's second law, the motion equation of the bicycle model is expressed as follows:

$$m(\dot{u}-rv)=F_{xf}+F_{xr} \quad (4)$$

$$m(\dot{v}+ru)=F_{yf}+F_{yr} \quad (5)$$

$$I_z\dot{r}=l_fF_{yf}-l_rF_{yr} \quad (6)$$

$$\dot{\psi}=r \quad (7)$$

$$\dot{X}=u\cos\psi-(v+ar)\sin\psi \quad (8)$$

$$\dot{Y}=u\sin\psi+(v+ar)\cos\psi \quad (9)$$

where the XOY is the global coordinate system and the xoy is the vehicle body-fixed coordinate system. $l_f, l_r$ denote the distance from CG to the front axle and rear axle and *u, v, r* are longitudinal speed, lateral speed and yaw rate at CG of the vehicle, respectively. $X, Y, \psi$ are the longitudinal position, lateral position and heading angle of the vehicle. *Fyf ,Fyr* are the lateral tire force of the front tires and rear tires and *Fxf ,Fxr* are the longitudinal force of the front tires and rear tires.

With the small angle assumption, the lateral tire force model could be linearized as

$$F_{yf}=C_f\alpha_f=C_f\left(\delta-\frac{v+l_fr}{u}\right) \quad (10a)$$

$$F_{yr}=C_r\alpha_r=C_r\left(-\frac{v-l_rr}{u}\right) \quad (10b)$$

where $\alpha_f, \alpha_r$ are the tire slip angle of the front tire and rear tire. $C_f, C_r$ denote the cornering stiffness values of the front and rear tires. $\delta$ is the steering wheel angle.

The relationship between the global coordinate system and the vehicle body-fixed coordinate system could be calculated by the rotation matrix as:

$$\begin{bmatrix}X_v\\Y_v\\\psi_v\end{bmatrix}=\begin{bmatrix}\cos\psi_i & \sin\psi_i & 0\\ \sin\psi_i & \cos\psi_i & 0\\ 0 & 0 & 1\end{bmatrix}\cdot\begin{bmatrix}X\\Y\\\psi\end{bmatrix}-\begin{bmatrix}X_i\\Y_i\\\psi_i\end{bmatrix} \quad (11)$$

### B. The NMPC Controller

MPC is commonly used in the path tracking control. Substituting (10) into (4)-(9), then the motion of the vehicle could be expressed as:

$$\begin{cases} m(\dot{u}-rv)=F_{xf}+F_{xr}\\ m(\dot{v}+ru)=C_f\left(\delta-\frac{v+ar}{u}\right)+C_r\left(-\frac{v-br}{u}\right)\\ I_z\dot{r}=aC_f\left(\delta-\frac{v+ar}{u}\right)-bC_r\left(-\frac{v-br}{u}\right)\\ \dot{X}=u\cos\psi-(v+ar)\sin\psi\\ \dot{Y}=u\sin\psi+(v+ar)\cos\psi \end{cases} \quad (12)$$

which could be written as:

$$\dot{\mathrm{X}}=f(\mathrm{X},u) \quad (13)$$

where $X=[\mathrm{X},\mathrm{u},\mathrm{Y},\mathrm{v},\psi,\dot{\psi}]^T$ are the state of the equation, the steering wheel angle and total longitudinal force are the control input $u=[\delta,F_x]^T$. The vehicle lateral position, heading angle and longitudinal speed are chosen to be the output of the equation as $Y=[\mathrm{Y},\psi,u]^T$.

Expanding the right side of equation (13) in Taylor series around the point $(x_0, u_0)$, it follows with discarding the high order as:

$$\dot{X} = f(X_0,u_0) + \underbrace{\left.\frac{\partial f}{\partial X}\right|_{X_0,u_0}}_{J(x)}(X - X_0) + \underbrace{\left.\frac{\partial f}{\partial u}\right|_{X_0,u_0}}_{J(u)}(u - u_0) \quad (14)$$

where $J(x)$ and $J(u)$ are the Jacobian matrix of $f(X,u)$ with respect to x and u around the point $(X_0,u_0)$.With the subtraction of equation(14), we can get the continues linearized model as:

$$\dot{\tilde{X}} = A\tilde{X} + Bu \quad (15)$$

In this formula, $\tilde{X} = X - X_0, \tilde{u} = u - u_0, Ac = J(x), B_c = J(u).$

For the NMPC，at each sampling time, the controller calculates a constrained finite time-optimal control problem, which could obtain an optimal control output sequence which minimizes the cost function under the constraints during the predict horizon. Take the first value of the output sequence as the input for the next sampling time and recalculate the optimization problem recursively.

So, the continuous state-space of vehicle model should be discretized as follows:

$$X(k+1) = A_d X(k) + B_d u(k) \quad (16)$$

$$Y(k) = C_d X(k) \quad (17)$$

where $A_d, B_d, C_d$ are the discrete state equations, which can be calculated as:

$$\begin{aligned} A_d &= I + A \cdot \Delta T \\ B_d &= B \cdot \Delta T \\ C_d &= C \end{aligned} \quad (18)$$

where $\Delta T$ is the sampling interval of the MPC controller, which is chosen as 10ms here.

In this paper, the prediction horizon is set as $N_p$ and the control horizon is set as $N_c$. Assuming the vehicle state is $X(k)$ at the current time k, the future state vector could be expressed with the current state and the future control input as:

$$\begin{aligned} (k+1) &= A_d X(k) + B_d u(k) \\ X(k+2) &= A_d X(k+1) + B_d u(k+1) \\ &= A_d^2 X(k) + A_d B_d u(k) + B_d u(k+1) \\ &\vdots \\ X(k+N_c) &= A_d^{N_c} X(k) + A_d^{N_c-1} B_d u(k) + \cdots \\ &\quad + B_d u(k+N_c-1) \\ &\vdots \\ X(k+N_p) &= A_d^{N_p} X(k) + A_d^{N_p-1} B_d u(k) + \cdots \\ &\quad + A_d^{N_p-N_c} B_d u(k+N_c-1) \end{aligned} \quad (19)$$

Then we can get the output during the predict horizon as:

$$Y_p(k) = C_p X(k) + D_p u_p(k) \quad (20)$$

where

$$Y_p(k) = \left[Y(k), Y(k+1)\ldots, Y(k+N_p)\right]^T$$

$$C_p = \left[C_d A_d, C_d A_d^2, \ldots C_d A_d^{N_p-1}\right]^T$$

$$D_p = \begin{bmatrix} C_d B_d & 0 & 0 & 0 & 0 \\ & & \vdots & & \\ C_d A_d^4 B_d & C_d A_d^3 B_d & C_d A_d^2 B_d & C_d A_d B_d & C_d B_d \\ & & \vdots & & \\ C_d A_d^{N_p-1} B_d & C_d A_d^{N_p-2} B_d & C_d A_d^{N_p-3} B_d & C_d A_d^{N_p-4} B_d & C_d A_d^{N_p-N_c} B_d \end{bmatrix}$$

The goal of the path tracking control is to minimize the tracking error between the actual path and desired trajectory with relative less control input. The desired trajectory includes reference lateral position $Y_r$, heading angle $\psi_r$ and speed $u_r$. So the cost function of the optimization problem could be defined as

$$\begin{aligned} J &= (Y - Y_r)^T q_1 (Y - Y_r) + (u - u_r)^T q_2 (u - u_r) + \\ &\quad (\psi - \psi_r)^T q_3 (\psi - \psi_r) + U^T r U \\ &= (Y_p - Y_{des})^T Q (Y_p - Y_{des}) + U^T r U \end{aligned} \quad (21)$$

Where $Y_{des}$ is the reference trajectory in prediction horizon $Np$, $Q = diag(q_1, q_2, q_3)$ denotes the weight vector of the tracking goals. $r$ is the control vector of future input. Substituting (20) into (21), the cost function could be written as the standard quadratic form as:

$$J = \frac{1}{2} U^T R U + f^T U \quad (22)$$

where

$$R = D_p^T Q D_p + \bar{R}$$

$$f = 2 D_p^T (C_p X(k) - Y_r)$$

However, there are some physical constrains of this optimization problem that both output and control variables could not violate. The constraint of output can be written as:

$$\begin{bmatrix} Y_{lb} \\ \psi_{lb} \\ u_{lb} \end{bmatrix} \le Y_p \le \begin{bmatrix} Y_{ub} \\ \psi_{ub} \\ u_{ub} \end{bmatrix} \quad (23)$$

where $Y_{lb}$ and $Y_{ub}$ are the boundaries for each side of the road to ensure the vehicle move in the structural road, $\psi_{lb}$ and $\psi_{ub}$ are the limit of the heading angle, $u_{lb}$ and $u_{ub}$ are the speed. Here, we do not have the heading angle limit and minimal speed limit. So set $u_{lb}$ equal to zero.

When steering at very high speed, vehicle sideslip may happen on the low-adhesion road and vehicle rollover may

happen on the high-adhesion road, which leads to the vehicle lose control. So steering at high speed is a very dangerous maneuver, especially for the vehicle has heavy mass and high mass centers such as SUV, buses, and trucks. To prevent the vehicle sideslip and rollover, the upper bound of the speed should be limited according to the road conditions.

*Sideslip constraint:* to prevent the vehicle sideslip, the lateral traction force should be restricted to the physical limitations of the tire-road friction. To simplify, the vehicle longitudinal acceleration and lateral acceleration is under the limit of the tire force as:

$$\sqrt{a_x^2 + a_y^2} \le \mu g \tag{24}$$

The whole lateral tire force is used to provide the centrifugal force under the steady-state steering condition, which is expressed as:

$$F_y = \frac{m V_x^2}{R} \tag{25a}$$

$$a_y \approx V_x^2 K \tag{25b}$$

Assume the tire force is totally applied for the lateral tire force, so the longitudinal force must be satisfied with:

$$V_x(s) \le \sqrt{\frac{a_y}{K(s)}} = \sqrt{\frac{\mu g}{K(s)}} \tag{26}$$

*Anti-rollover constraint:* when vehicle steers at the high speed, the lateral acceleration causes the load transfer. Too much load transfer causes the lower loaded side lose its adhesion. At that moment, vehicle rollover happens. To prevent rollover, severe load transfer caused by lateral acceleration should be restricted.

According to the vehicle longitudinal dynamics, the total longitudinal resistance force could be calculated as:

$$F_r = m \cdot g \left( f \cdot \cos\alpha + \sin\alpha \right) \tag{27}$$

where $F_r$ is the longitudinal resistance force, $f$ is the road rolling resistance coefficient and $\alpha$ is the incline angle of the road. To simplify, the wind resistance force is neglected.

For a 4-wheel-driven electric vehicle, four wheels generate equal longitudinal force to overcome the resistance force when the vehicle moves under steady-state conditions. Once load transfer happens, less load at lower loaded side could be utilized to produce the longitudinal force[10]. By calculating the load transfer, the anti-rollover constraint could be expressed as:

$$\mu \left( \frac{m \cdot g}{2} - \frac{m \cdot h_g \cdot |a_y|}{w} \right) \ge \frac{F_r}{2} \tag{28}$$

where $h_g$ represents the centroid height and $\mu$ is road adhesion coefficient. Combining (27) and (28), the speed limit of anti-rollover is given as:

$$v_{rl} = \sqrt{\frac{\left( m \cdot g - \frac{F_r}{\mu} \right) \cdot w}{2m \cdot h_g \cdot K}} \tag{29}$$

To sum up, the upper bound of the velocity is:

$$v_{ub} = S \cdot \min\left( v_{sl}, v_{rl}, v_{\max} \right) \tag{30}$$

where $S$ is positive safety factor which is less than 1 and $v_{max}$ is legal maxim vehicle speed.

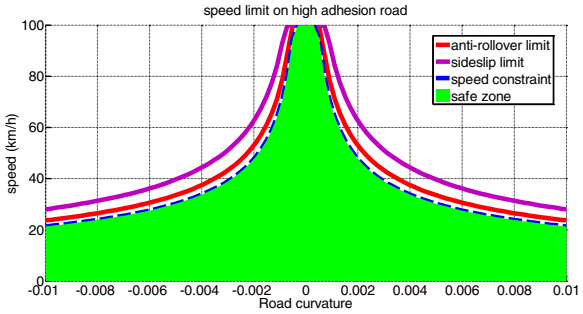


Fig. 3. The speed limit on high adhesion road

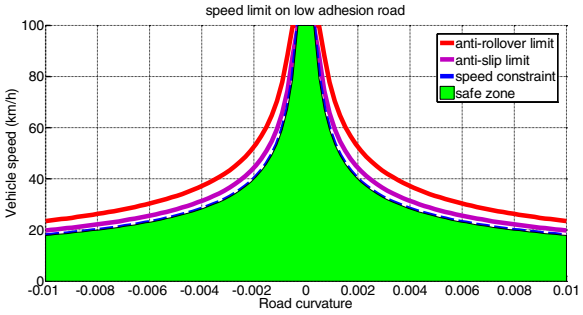


Fig. 4. The speed limit on low adhesion road

Fig.3 and Fig.4 illustrate the upper bound limit of longitudinal speed limit under the road adhesion coefficient of 0.8 and 0.4, respectively. It is obvious that the upper bound of the vehicle speed is restricted by the anti-rollover limit on the high-adhesion road and that is restricted by the anti-slip limit on the low-adhesion road.

For the control input, they also must obey the physical limit of the actuators, which could be expressed as:

$$\begin{bmatrix} \delta_{lb} \\ F_{xlb} \end{bmatrix} \le u \le \begin{bmatrix} \delta_{ub} \\ F_{xub} \end{bmatrix} \tag{31}$$

$$\begin{bmatrix} \Delta\delta_{lb} \\ \Delta F_{xlb} \end{bmatrix} \le \Delta u \le \begin{bmatrix} \Delta\delta_{ub} \\ \Delta F_{xub} \end{bmatrix} \tag{32}$$

where $\delta_{lb}, \delta_{ub}, F_{xlb}, F_{xub}$ are the constraints of the steering wheel angle and longitudinal force, and $\Delta\delta_{lb}, \Delta\delta_{ub}, \Delta F_{xlb}, \Delta F_{xub}$ represent the change rate of control input, which is determined by the physical properties of the steering motor and wheel motors.

With all the constraints above, the optimization problem with constraints can be summed up by:

$$\min J = \frac{1}{2}\left(Y_p - Y_{des}\right)^T Q\left(Y_p - Y_{des}\right) + U^T \bar{R} U$$

*Subject to* :

$$X(k+1) = A_d X(k) + B_d U(k)$$
$$Y_p = C_p X(k) + D_p U_p(k) \quad (33)$$
$$I_{3Np\times 1} Y_{\min} \le Y_p \le I_{3Np\times 1} Y_{\max}$$
$$I_{2Nc\times 1} u_{\min} \le U_p(k) \le I_{2Nc\times 1} u_{\max}$$
$$I_{2Nc\times 1} \Delta u_{\min} \le U_p(k) - U_p(k-1) \le I_{2Nc\times 1} \Delta u_{\max}$$

In this paper, the Matlab embedded function 'quadprog' is adopted to solve this SQP problem to obtain the optimal steering wheel angle and total longitudinal force. The real input of the vehicle is steering wheel angle and wheel motor torque, which could be calculated through optimal torque vectoring method with the desired wheel angle and total longitudinal force[11].

## IV. SIMULATION RESULTS AND ANALYSIS

To evaluate the effectiveness of the proposed control algorithm, the simulation platform is established for the 4-wheel-drive electric SUV based on the Carsim software, the numerical solution of the optimization problem is conducted by Matlab/Simulink software. The vehicle parameters are shown in TABLE I.

TABLE I. VEHICLE PARAMETERS

| **Vehicle Parameters** | | |
|---|---|---|
| ***Symbol*** | ***Value*** | ***Unit*** |
| $m$ | 2300 | Kg |
| $a$ | 1350 | mm |
| $b$ | 1600 | mm |
| $w$ | 1800 | mm |
| $C_f$ | 60000 | N/deg |
| $C_r$ | 60000 | N/deg |
| $I_z$ | 3500 | Kg*m$^2$ |

Here, two simulation cases are designed to illustrate the desired performance of proposed control algorithm under different road conditions.

Case 1: The sharp lane change maneuver at high speed on the concrete road. The initial vehicle speed is 80km/h and the road adhesion coefficient is $\mu = 0.9$.

Case 2: The lane keeping on the 'S-turn' shaped road with paved snow. The initial vehicle speed is 35km/h and the road adhesion coefficient is $\mu = 0.5$.

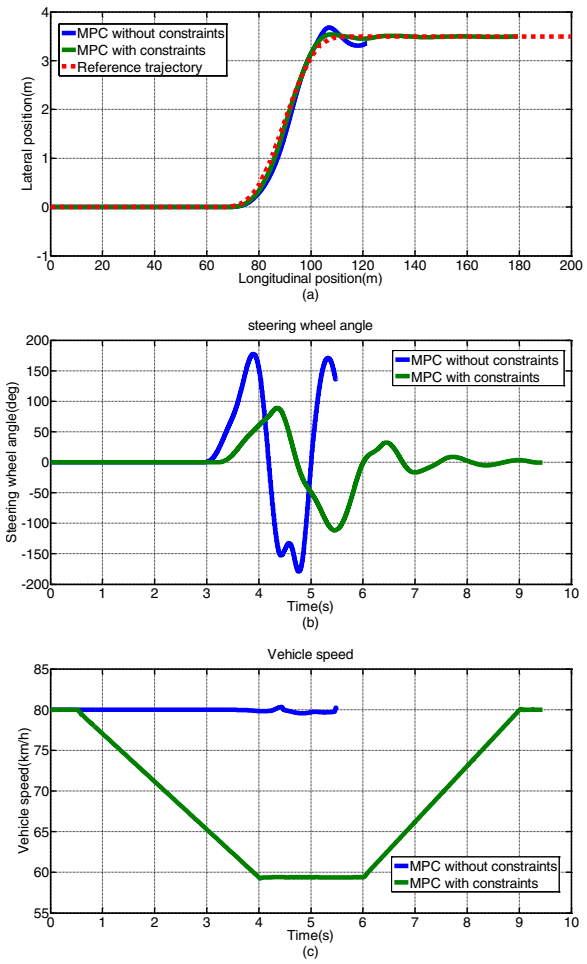


Fig. 5. Simulation results of case 1

Fig.5 illustrates the comparison of the control effect of MPC path tracking controller. For the MPC without control, it always keeps the initial speed of 80km/h. when the vehicle begins to steer, lateral acceleration increases which leads to load transfer. At the time of 5.14, the outer wheel begins to lose adhesion and at the time of 5.67, rollover happens. For the MPC with speed constraints, the vehicle decelerates before it starts to steer and always keep its speed in the safe zone. So this controller keeps vehicle stable and has satisfactory tracking performance.

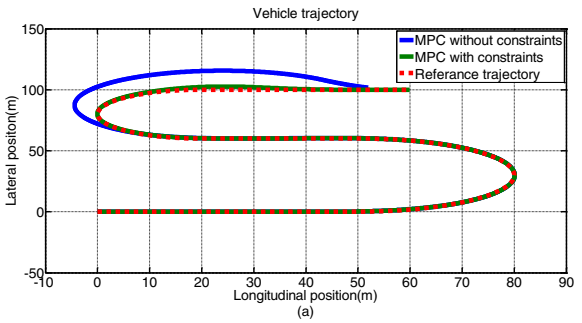

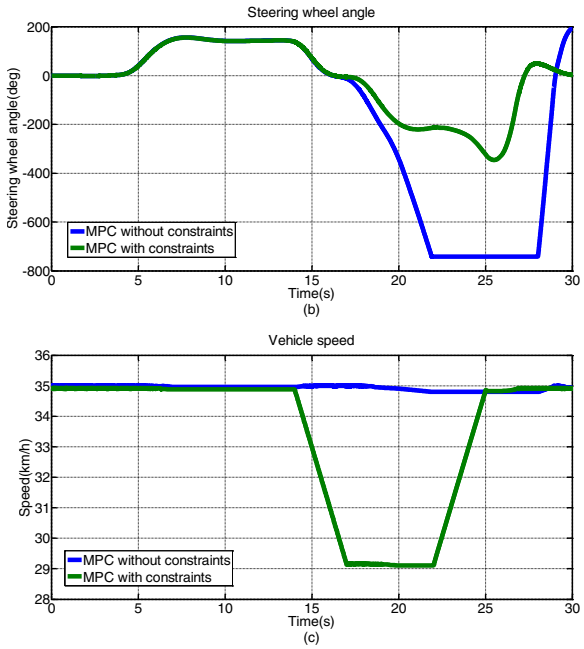


Fig. 6. Simulation results of case 2

Fig.6 shows the control effects of these two controllers on low adhesion road. The "S-turn" road has two turns with the radius of 30m and 20m, respectively. For the MPC without control, it can pass the first turn successfully. But when it comes to the second turn, the wheel force reaches the limit of adhesion. The lateral force no longer increases with more steering wheel angle. At this time, vehicle sideslip happens which leads the vehicle deviates the reference path. For the MPC with speed control, it reduces the vehicle speed before entering the second turn. The tire force is always under adhesion limit to prevent the vehicle sideslip. So it has higher tracking accuracy.

## V. CONCLUSION

This paper proposed an application of model predictive control for vehicle path tracking. Based on the known road information, the convex optimization problem is established to minimize the tracking error. Meanwhile, the constraints for optimization are also considered by analyzing the vehicle lateral stability. The simulation results demonstrate that the proposed control algorithm has satisfactory tracking performance and could effectively prevent the vehicle sideslip and rollover on low adhesion and high adhesion road to keep the vehicle safe.

## REFERENCES

[1] R. C. Rafaila and G. Livint, "Nonlinear model predictive control of autonomous vehicle steering," in *System Theory, Control and Computing (ICSTCC), 2015 19th International Conference on*, 2015, pp. 466-471.

[2] J. Nilsson, Y. Gao, A. Carvalho, and F. Borrelli, "Manoeuvre generation and control for automated highway driving," *IFAC Proceedings Volumes,* vol. 47, pp. 6301-6306, 2014.

[3] O. Montiel, U. Orozco-Rosas, and R. Sepúlveda, "Path planning for mobile robots using Bacterial Potential Field for avoiding static and dynamic obstacles," *Expert Systems with Applications,* vol. 42, pp. 5177-5191, 2015.

[4] S. Salehpour, Y. Pourasad, and S. H. Taheri, "Vehicle path tracking by integrated chassis control," *Journal of central south university,* vol. 22, pp. 1378-1388, 2015.

[5] Y. Luo, Y. Xiang, K. Cao, and K. Li, "A dynamic automated lane change maneuver based on vehicle-to-vehicle communication," *Transportation Research Part C: Emerging Technologies,* vol. 62, pp. 87-102, 2016.

[6] L. Wang, Model predictive control system design and implementation using MATLAB®: Springer Science & Business Media, 2009.

[7] J. Ji, A. Khajepour, W. W. Melek, and Y. Huang, "Path Planning and Tracking for Vehicle Collision Avoidance Based on Model Predictive Control With Multiconstraints," *IEEE Transactions on Vehicular Technology,* vol. 66, pp. 952-964, 2017.

[8] Y. Rasekhipour, A. Khajepour, S.-K. Chen, and B. Litkouhi, "A Potential Field-Based Model Predictive Path-Planning Controller for Autonomous Road Vehicles," *IEEE Transactions on Intelligent Transportation Systems,* vol. 18, pp. 1255-1267, 2017.

[9] J. Funke, M. Brown, S. M. Erlien, and J. C. Gerdes, "Collision avoidance and stabilization for autonomous vehicles in emergency scenarios," *IEEE Transactions on Control Systems Technology,* vol. 25, pp. 1204-1216, 2017.

[10] W. Liu, H. He, F. Sun, and J. Lv, "Integrated chassis control for a three-axle electric bus with distributed driving motors and active rear steering system," *Vehicle System Dynamics,* vol. 55, pp. 601-625, 2017.

[11] L. Zhai, T. Sun, and J. Wang, "Electronic Stability Control Based on Motor Driving and Braking Torque Distribution for a Four In-Wheel Motor Drive Electric Vehicle," *IEEE Transactions on Vehicular Technology,* vol. 65, pp. 4726-4739, 2016.